Rock and Soil Mechanics

Volume 42 | Issue 8 Article 1

12-16-2021

Experimental study on the strength characteristics of a transparent cemented soil

Xian-lun LENG
University of Chinese Academy of Sciences, Beijing 100049, China

Chuan WANG
University of Chinese Academy of Sciences, Beijing 100049, China

Rong PANG
College of Civil Engineering and Environment, Hubei University of Technology, Wuhan, Hubei 430068, China

Qian SHENG
University of Chinese Academy of Sciences, Beijing 100049, China

Custom Citation

LENG Xian-lun, WANG Chuan, PANG Rong, SHENG Qian, . Experimental study on the strength characteristics of a transparent cemented soil[J]. Rock and Soil Mechanics, 2021, 42(8): 2059-2068.

Rock and Soil Mechanics 2021 42(8): 2059−2068 ISSN 1000−7598
https: //doi.org/10.16285/j.rsm.2021.5181 rocksoilmech.researchcommons.org/journal

Experimental study on the strength characteristics of a transparent cemented soil

LENG Xian-lun[1, 2], WANG Chuan[1, 2], PANG Rong[3], SHENG Qian[1, 2]

1. State Key Laboratory of Geomechanics and Geotechnical Engineering, Institute of Rock and Soil Mechanics, Chinese Academy of Sciences, Wuhan, Hubei 430071, China

2. University of Chinese Academy of Sciences, Beijing 100049, China

3. College of Civil Engineering and Environment, Hubei University of Technology, Wuhan, Hubei 430068, China

Abstract: The visual physical model testing technology based on transparent soils is playing an increasingly important role in the study of deformation and failure mechanism in geotechnical engineering. The preparation of transparent soils with high transparency, stable physical and mechanical properties, and suitable for simulating different natural rocks and soils is the basis for the development of this technology. Given the lack of transparent materials for clays and soft rocks, a transparent cemented soil has been formulated. The transparent cemented soil is synthesis using fused quartz as the skeleton particles, nano-level hydrophobic fumed silica powder as the cement and mixed mineral oil of n-dodecane and #15 white oil as the pore fluid. By changing the content or proportion of the cement, the particle size or gradation of the skeleton, a series of transparent cemented soils with similar refractive index and varying strength characteristics can be obtained. For the factors influencing the soil strength, such as cement content and skeleton gradation, 11 groups of controlled experiments were designed and corresponding triaxial shear tests were conducted to study the strength characteristics. Results show that: 1) The shear strength varies complexly with the changes of the particle size and gradation of the fused quartz, the content and proportion of the silica powder, etc., but overall the poor quality of quartz gradation and the rich proportion of silica powder reduces the shear strength. 2) By changing the preparation formulas, a series of transparent cemented soils with cohesions ranging from 5 to 65 kPa and internal friction angles ranging from 25° to 44° can be prepared, which provides a basis for the selection and preparation of transparent materials in physical model experiments using natural clays and soft rocks.

Keywords: transparent cemented soil; preparation method; fused quartz; hydrophobic fumed silica powder; triaxial shear test; strength characteristics

1 Introduction

The observation of deformation, failure and seepage process in rock and soil mass is an important way of indoor model tests to reveal the catastrophic evolution mechanism in geotechnical engineering. Model tests using traditional geotechnical materials make it difficult to observe the evolution process of internal deformation and failure of the rock and soil mass, which is not conducive to the study of the mechanical mechanism of disasters. To solve this problem, researchers developed a set of visual test technology based on transparent soils, which used transparent soils instead of natural soils to carry out model tests and combines this with optical image processing technology to realize the visualization of the internal deformation and disaster evolution process of the rock and soil mass[1−2]. The basis of this technology is the preparation of transparent soil materials with high transparency, similar mechanical and hydraulic properties to natural rocks and soils.

At present, two methods are commonly used to artificially synthesize transparent soils[3−4].

One uses the transparent soil (type 1) synthesized with amorphous silica fume (micron level) as the soil skeleton, and its geotechnical properties are similar to soft clay[5]. Iskander et al.[5−7] used 4 kinds of amorphous silica powders with different particle sizes (particle sizes are 1.4, 10, 25, and 175 μm) to make transparent soft clay and obtained the mechanical properties through triaxial tests, showing that the internal friction angle under high confining pressure is 19°–36°, and the cohesion is 0–16 kPa. Subsequently, Wu et al. [8], Lei et al.[9] changed the particle size or grade of amorphous silicon powder to further study the mechanical properties of this kind of transparent soft clay. The study showed that the cohesion of this kind of transparent soft clay under low confining pressure is about 10 kPa, and the internal friction angle is 14°–18°. This kind of transparent soft clay is mainly used in the physical model test research, such as soft clay pile driving process[10], soft clay foundation consolidation and drainage [11].

The second method uses transparent soil synthesized with amorphous silica gel (millimeter level) or fused silica sand (millimeter level) as the soil skeleton (type 2), and its geotechnical properties are similar to sandy soil[12−13]. Sadek et al.[13] and Iskander et al.[12] synthesized transparent sands with amorphous silica gel with an internal friction angle of 30°–36°. Kong et al.[14−15] used fused silica sand to make a transparent sand with an internal friction angle of about 40°–45°. These two kinds of transparent sands have no cohesion or low cohesion (⩽1 kPa), and are mainly used for soil deformation around cast-in-place piles and uplift piles[16−17], the stability of excavation surface of circular tunnel and the inrush of water and mud[18−19], the deformation of generalized slope under action of

Received: 2 February 2021 Revised: 4 March 2021
This work was supported by the National Key R&D Program of China (2017YFF0108705) and the National Natural Science Foundation of China (52079135).
First author: LENG Xian-lun, male, born in 1980, PhD, Associate Professor, research interests: geotechnical engineering and stability. E-mail: xlleng@whrsm.ac.cn

water[20–21], the pore flow characteristics of porous media[22–23] and other physics model test research.

The above two types of synthetic transparent soils both use a mixed liquid with the same refractive index as the soil skeleton as the pore liquid. The currently commonly used pore liquid is a mixed mineral oil of n-dodecane and #15 white oil, calcium bromide solution (solid calcium bromide is soluble in water) [24–25].

Because the above two types of synthetic transparent soils have the disadvantages of low strength (type 1) or weak cohesion (type 2), they can only be used to simulate a few specific rock and soil mass, and it is difficult to create physical models with more complex shapes, such as slopes with large slope angles, foundation pits, caverns. Therefore, the preparation of transparent soils with the similar strength of general geotechnical materials is of great significance to the development of related model tests. Wei et al.[26–27] combined the advantages of the two methods for preparing transparent soils and synthesized a transparent cemented soil, using fused quartz as the soil skeleton, silica powder as the cement, and mixed mineral oil as the pore fluid. They proved that its mechanical and hydraulic characteristics are suitable for simulating general clays. However, there is a lack of further research on the quantitative ratio of the components in the transparent cemented soil, the particle size and gradation of fused quartz, and the degree of compaction of the transparent cemented soil, and it is difficult to directly apply it to the physical model.

In this paper, we learned from the idea of Wei et al.[26–27] in making transparent cemented soil and added a kind of hydrophobic fumed silica powder (nano-level) as a cement into the transparent sand made by Kong et al.[14–15] to synthesize a new transparent cemented soil. By controlling the content and proportion of fused quartz and silica powder, and the particle size and gradation of fused quartz, the transparent cemented soil shows a similar shear strength with ordinary clays or soft rocks. Furthermore, 11 groups of testing schemes with different cement ratios were designed according to the influence factors such as the content and gradation of the components, and unconsolidated and undrained triaxial shear tests were carried out to study the influence of different ratios on the shear strength parameters and their relationships. A reasonable preparation method of transparent cemented soil suitable for clays and soft rocks is given, which can provide a basis for similar material preparation of transparent soil for natural clays and soft rocks in physical model tests of geotechnical engineering.

2 Preparation of transparent cemented soil

2.1 Raw materials

The raw materials of the transparent cemented soil prepared in this paper and their functions: fused quartz as the soil skeleton, mixed mineral oil of n-dodecane and #15 white oil as the pore fluid, and nano-level hydrophobic fumed silica powder as the cement.

The fused quartz used (see Fig.1(a)) is divided into 3 groups according to the particle size, which are 0.2–0.5, 0.5–1.0, 1.0–2.0 mm. The specific gravity of each group of the fused quartz is 2.2, and the refractive index is 1.458 5. In the natural state, the dry densities of the three groups of fused quartz deposits are 1.40, 1.25, and 1.10 g/cm^3, and the porosities are 36%, 43%, and 50%. After being compacted by hydraulic jacks and unloading and rebounding, the maximum dry density of the fused quartz can reach 1.65, 1.55, and 1.40 g/cm^3, and the porosity are 25%, 30%, and 36%, respectively.

The nano-level hydrophobic fumed silica powder (see Figure 1(b)) used is a modified silica. It looks like white powder, with a particle size of ⩽15 nm and a bulk density of about 70 g/L in the natural state. It has a large specific surface area and good dispersion. The refractive index of the silica powder is the same as that of fused quartz (1.458 5), so mixing it with fused quartz and mixed mineral oil will not change the transparency of the material. At the same time, the size of the silica powder is nanoscale, with special properties such as small size effect and surface effect. In addition, the silica powder has hydrophobic (lipophilic) properties and can absorb mixed mineral oil. Therefore, after being mixed with fused quartz and mixed mineral oil, the silica powder can be adsorbed to the surface of the fused quartz, so that the fused quartz can be bonded to each other and exhibits the properties of clay particles.

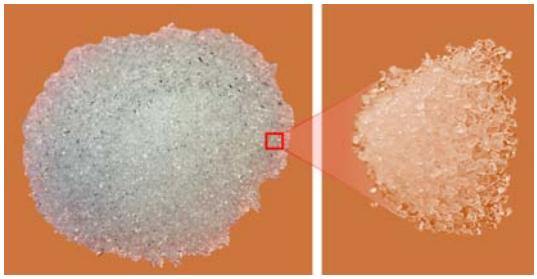

(a) Soil skeleton: fused quartz

(b) Cement: hydrophobic fumed silica powder

Fig. 1 Skeleton and cement of the transparent soil

In order to make the mixed transparent cemented soil achieve better transparency and prevent light from refraction between the pores and the skeleton, it is necessary to prepare a pore fluid, the refractive index (1.458 5) of which is consistent with that of fused quartz and silica powder. The pore fluid used in this paper is a mixed mineral oil of n-dodecane and #15 white oil. In an environment of 26℃, the refractive index of n-dodecane is 1.424, and the refractive index

of #15 white oil is 1.469. The refractive index of the pore fluid increases with the increase of temperature. Generally speaking, the refractive index of mixed mineral oil and that of fused quartz is the same or close when the proportion of n-dodecane to #15 white oil is 1:3.5–1:8. When the refractive index is high, the refractive index of the mixed mineral oil can be reduced by adding n-dodecane, and when the refractive index is low, the refractive index can be increased by adding #15 white oil.

2.2 Preparation process

The preparation process of the transparent cemented soil is divided into the following 5 steps:

(1) Prepare mixed mineral oil of n-dodecane and #15 white oil to make the refractive index 1.458 5; wash and dry the fused quartz to remove impurities and moisture on the surface, and seal it for later use.

(2) Determine the mixing ratio of fused quartz (skeleton), silica powder (cement) and mixed mineral oil (pore fluid). For the convenience of subsequent expressions, the proportion of silica powder to fused quartz is defined as the "proportion of silica powder". Several tests have shown that the proportion of silica powder in transparent cemented soil should be 2%–20%, and the transparent cemented clay with different proportion of silica powder have different mechanical properties. In order to facilitate evenly mixing and compaction, the mass of the mixed mineral oil m_{oil} can be determined by the mass of fused quartz m_{qtz} and the mass of silica powder m_{slc}:

$$m_{\mathrm{oil}} = 0.05m_{\mathrm{qtz}} + 2.5m_{\mathrm{slc}} \quad (1)$$

where $0.05m_{\mathrm{qtz}}$ represents the minimum amount of mixed mineral oil required for wetting dry fused quartz, and $2.5m_{\mathrm{slc}}$ represents the minimum amount of mixed mineral oil required to saturate the silica powder.

(3) Mix the fused quartz, silica powder and mixed mineral oil to make the silica powder adsorb to the surface of the fused quartz particles. Different fused quartz particles are bonded to each other through the silica powder to form a block structure with different sizes. The mixture is pale white at this time, as shown in Fig. 2(a).

(4) The cemented soil block is compacted in layers, and the surface is roughened after each compaction, and then the next compaction is performed, and the compaction height of each layer should not exceed 3 cm, and the maximum compaction degree can be made 87%–95% of the cemented soil. At this time, the saturation of the cemented soil is 75%–85%. Because it is not fully saturated, the cemented soil is light milky white or colorless and translucent, as shown in Fig.2(b).

(5) Put the cemented soil obtained from the previous step into a vacuum box to exhaust for 5–6 hours, and then add an appropriate amount of mixture of mineral oil to back pressure and saturate it for 1–2 hours to fully saturate the cemented soil. The fully saturated cemented soil is colorless and transparent, as shown in Fig. 2(c).

(a) Mixture of fused quartz, silica powder and mixed mineral oil

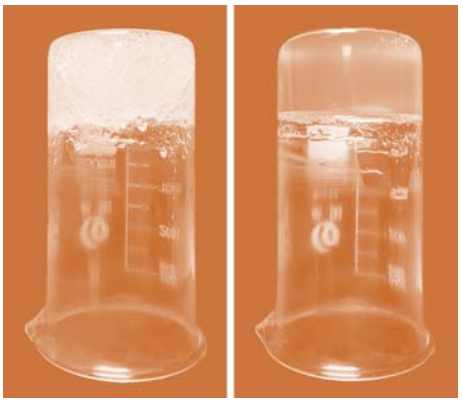

(b) Unsaturated cemented soil (c) Fully saturated cemented soil

Fig. 2 Preparation process of the transparent cemented soil

It is worth noting that:

(1) In the material preparation process, the degree of compaction has a greater influence on the mechanical properties of transparent cemented soil. The main factors affecting the maximum degree of compaction of transparent cemented soil are the particle size and gradation of fused quartz, the content of silica powder and the content of mixed mineral oil. Among them, the particle size and gradation of fused quartz and the content of silica powder are usually determined according to the mechanical properties of the transparent cemented soil to be prepared. In this case, in order to facilitate compaction, the content of mixed mineral oil is determined according to Eq. (1).

(2) Fused quartz, silica powder and mixed mineral oil are not easy to mix evenly after mixing. For this reason, we summarized a set of empirical methods for mixing in the operation: ①When the proportion of silica powder is ≤10%, first wet the fused quartz and the mixed mineral oil at a proportion of 20:1, then add silica powder and stir thoroughly. When the silica powder is uniformly adsorbed to the surface of the fused quartz, add 2.5 times the mass of the mixed mineral of the silica powder and mix with oil to fully saturate the silica powder. ②When the proportion of silica powder is> 10%, first mix the silica powder with all the mixed mineral oil to fully saturate the silica powder to form a transparent gel, then add fused quartz to mix so that the silica powder is evenly adsorbed on the fused quartz particles.

(3) Due to the smaller size and lower bulk density of fumed silica power particles, it is easy to float in the air during the mixing process. A large amount of inhalation of silica powder will cause certain damage to the

lungs, so wearing face masks is recommended during the mixing process.

3 Testing method

3.1 Sample preparation and testing

In order to test the shear strength parameters of the transparent cemented soil, a series of unconsolidated and undrained (UU) triaxial shear tests was carried out. The test was carried out on the soil triaxial shear instrument (model: SJ-1A) of the Institute of Rock and Soil Mechanics, Chinese Academy of Sciences. The sample size is 39.1 mm (diameter) × 80 mm (height), and the loading rate is 0.368 mm/min. Put the prepared uniform mixture of fused quartz, silica powder and mixed mineral oil into a sample preparation instrument according to a certain amount for compaction and sample preparation. A sample of transparent cemented soil with degree of compaction of 84% to 93% and degree of saturation of about 80% can be obtained. Since the sample is not fully saturated, the sample is translucent or pale white at this time, as shown in Fig. 3.

Fig. 3 Sample of the transparent cemented soil

In order to make the transparent cemented soil show better transparency, it should be ensured that the transparent cemented soil is fully saturated in the model test. Therefore, understanding the mechanical properties of the saturated transparent cemented soil is the basis of the transparent soil test. However, due to the limitation of the test conditions, this paper failed to carry out the triaxial test of saturated transparent cemented soil. Only the unsaturated sample with a degree of saturation of 80% was used instead of the saturated sample to carry out the UU test. The reasons are as follows:

(1) As is known to all, it is necessary to perform consolidated undrained (CU) or consolidated drained (CD) tests on saturated soil samples to measure their shear strength parameters. However, in the process of consolidation or drainage of saturated transparent cemented soil samples, the pore fluid (mixed mineral oil) discharged from the sample will corrode rubber products (such as latex membrane, sealing rubber ring), resulting in test failure and even damage to the instrument. Figure 4 is the comparison of the latex membrane of the soil sample before soaking and after soaking for 12 hours in the mixed mineral oil . It can be seen from the figure that the color of the latex membrane after the corrosion of the mixed mineral oil becomes lighter (actually the latex membrane becomes thinner). The diameter and length of the latex membrane both increase.

(2) Although the transparent cemented soil used in the model test is completely saturated, the excess static pore pressure in the model can almost be ignored due to the small size of these models (usually the maximum size does not exceed 60 cm). In the case of ignoring the pore pressure, the mechanical properties of an unsaturated transparent soil with a degree of saturation of 80% are similar to those of a fully saturated transparent soil. Therefore, an unsaturated soil sample with a higher degree of saturation can be used to approximately replace the saturated soil sample for testing.

Fig. 4 Comparison of latex films before and after corrosion of mixed mineral oil

3.2 Testing plan

In order to study the influence of content and proportion of silica powder, and particle size and gradation of fused quartz on the mechanical properties of transparent cemented soil, transparent cemented soils with different contents and proportions of silica powder and different particle sizes and gradations of fused quartz were prepared. Unconsolidated and undrained (UU) triaxial shear tests were carried out on the soil. The content of mixed mineral oil in the sample is determined by Eq. (1), and all samples are fully compacted. Considering that the confining pressure of the transparent soil in the model test is usually low, in order to make the stress conditions in the triaxial shear test match the model test as much as possible, the confining pressures set for this triaxial shear test are also relatively low, at 50, 100, 200 kPa, respectively. When the proportion of silica powder is less than 2%, the viscosity of the transparent cemented soil is extremely low, and the sample is difficult to be formed. Therefore, the proportion of silica powder in the transparent cemented soil studied in this paper is $\geqslant$2%.

The basic information of the test plan and sample is shown in Table 1, where

(1) The fused quartz content of the samples in the test groups G1 and G2 are both 1.380 g/cm^3, and the silica powder content is 0.028 g/cm^3 and 0.041 g/cm^3, respectively. Therefore, the test groups G1 and G2 constitute a control group with a constant content of fused quartz and the content of silica powder as a variable.

(2) The proportions of silica powder in the samples

in the test groups G3–G6 are 5%, 7%, 10% and 15% respectively, and the degree of compaction, saturation and other conditions are basically the same, so the test groups G3–G6 constitute a control group with the proportion of silica powder as a variable under constant degree of compaction and saturation.

(3) The masses of the fused quartz and silica powder of the samples in the test groups G5, G7 and G8 are the same, only the particle size of the fused quartz (respectively 0.5–1.0, 0.2–0.5, 1.0–2.0 mm) is different. Therefore, the test groups G5, G7 and G8 constituted a control group with fused quartz particle size as a variable.

(4) The contents of fused quartz and silica powder of the samples in the test groups G9, G10 and G11 are the same, only the particle gradation of the fused quartz (0.2–1.0, 0.2–2.0, 0.5–2.0 mm respectively) is different. Therefore, the test groups G9, G10, and G11 constitute a control group with fused quartz particle gradation as a variable.

Table 1 Testing plan and basic information of each group of samples

Test group	Proportion of silica powder to fused quartz /%	Particle size of fused quartz /mm	Content of each ingredient /(g • cm^{-3})			Degree of compaction /%	Bulk density /(g • cm^{-3})
			Fused quartz	Silica powder	Mixed mineral oil		
G1	2	0.5～1.0	1.378	0.028	0.138	84 (maximum)	1.55
G2	3	0.5～1.0	1.378	0.041	0.172	89 (maximum)	1.59
G3	5	0.5～1.0	1.240	0.062	0.217	91 (maximum)	1.52
G4	7	0.5～1.0	1.135	0.079	0.256	92	1.47
G5	10	0.5～1.0	0.992	0.100	0.297	92	1.39
G6	15	0.5～1.0	0.826	0.124	0.351	93	1.30
G7	10	0.2～0.5	0.992	0.100	0.297	92	1.39
G8	10	1.0～2.0	0.992	0.100	0.297	92	1.39
G9	10	0.2～1.0	0.992	0.100	0.297	92	1.39
G10	10	0.2～2.0	0.992	0.100	0.297	92	1.39
G11	10	0.5～2.0	0.992	0.100	0.297	92	1.39

4 Strength characteristics

4.1 Influence of silica powder content

In the case of a constant fused quartz content, the strength characteristics of samples with different silica powder content are shown in Fig. 5. The two sets of data in Figs. 5(a) and 5(b) where the proportion of silica powder is 2% and 3% respectively correspond to the G1 and G2 tests in Table 1. The contents of fused quartz in these two sets of samples are both 1.378 g/cm^3, and the silica powder content is 0.028 g/cm^3 (G1 group, silica powder accounts for 2%) and 0.041 g/cm^3 (G2 group, silica powder accounts for 3%). The data of group G0 in Fig.5(c) is extracted from the study of Kong et al.[14–15]. The test conditions of this group are similar to those of groups G1 and G2 in this paper. The main difference lies in the silica powder in this group of samples. The content of the silica powder is 0.

(1) In the case of a constant fused quartz content, the increase in the content of silica powder has basically no effect on the shape of the stress–strain curve and the position of the inflection point of the sample; under the same strain condition, the sample with a higher content of silica powder exhibits a relatively large stress, and this phenomenon is particularly pronounced when the confining pressure is low (50 kPa) (see Fig. 5(a)).

(2) Under the same confining pressure conditions, the samples with higher silica powder content correspond to larger Mohr circles, and the samples show higher strength; the strength envelopes of samples with different silica powder contents are approximately parallel, indicating that the content of silica powder mainly affects the cohesion of the sample, but has a small effect on the angle of internal friction (see Fig.5(b)).

(3) With the increase of silica powder content, the cohesive force of the sample increases significantly, while the internal friction angle increases slowly; the silica powder content in the sample increases from 0 to 0.028 g/cm^3 (accounting for 2% of the proportion of fused quartz) and 0.041 g/cm^3 (accounting for 3% of the proportion of fused quartz), the cohesion increases from 0 to 34 kPa and 66 kPa, and the internal friction angle increases from 38° to 43 ° and 44° (see Fig. 5(c)).

4.2 Influence of proportion of silica powder

Under the conditions of constant degree of compaction and saturation, the strength characteristics of samples with different proportions of silica powder are shown in Fig. 6. In the figure, the four sets of data with the proportion of silica powder being 5%, 7%, 10% and 15% respectively correspond to the G3–G6 group tests in Table 1. The degree of compaction of the samples in these four groups of tests are all 91%–93%, the degree of saturation is about 80%. Although the bulk density and the content of the mixed mineral oil of the 4 groups of samples are different, the bulk density of the samples and the content of the mixed mineral oil do not change independently but change together with the proportion of silica powder. Therefore, the 4 groups of tests can still be considered as a control experiment with the proportion of silica powder as a single variable. In the same way, in order to ensure the consistency of the degree of compaction of each group of samples, as the proportion of silica powder increases, the proportion of fused quartz in the sample decreases accordingly (see Fig. 6(c)).

Figures 6(a) and 6(b) both take the two sets of samples with 5% and 10% silica powder as examples to illustrate how the stress–strain curve and strength envelope of the samples change with different silica powder ratios. The other samples with the proportion of silica powder show similar laws, and the change rule of the strength parameter with the proportion of silica power is shown in Fig. 6(c). The figure shows:

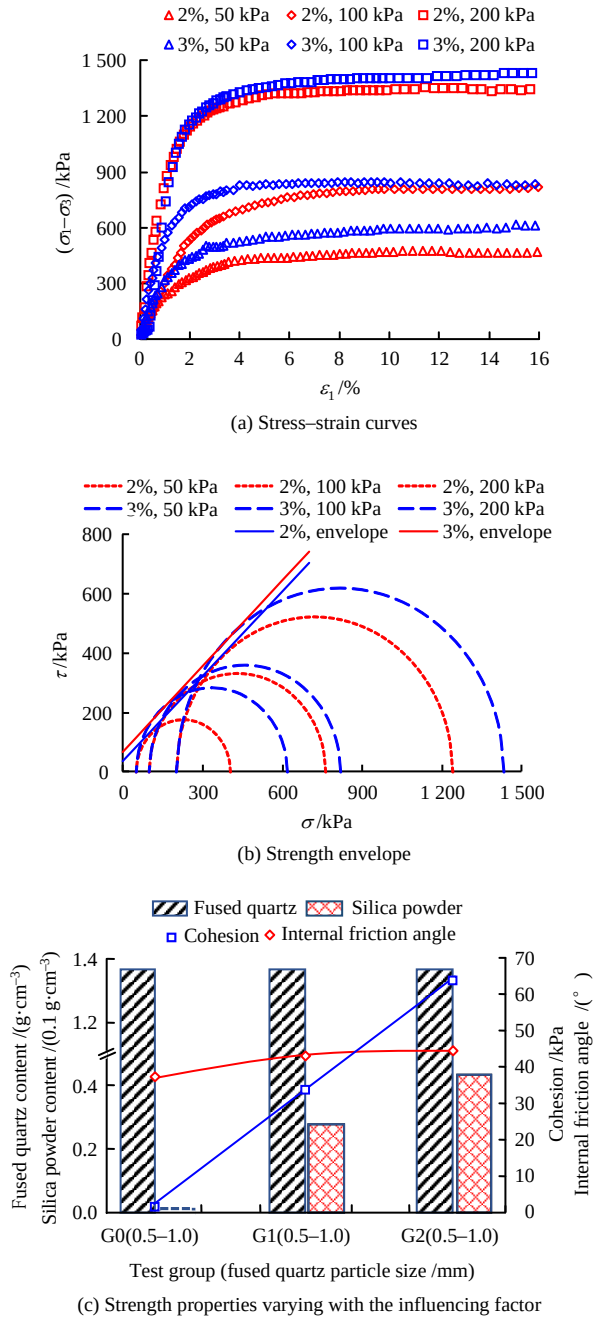

(a) Stress–strain curves

(b) Strength envelope

(c) Strength properties varying with the influencing factor

Fig. 5 Strength characteristics of samples with different contents of silica powder

(1) In the case of constant degree of compaction, the increase in the proportion of silica powder has basically no effect on the shape of the sample stress–strain curve, and the position of the inflection point of the curve slightly advances with the increase in the proportion of silica powder. For example, under a confining pressure of 200 kPa, the inflection point of the sample with 5% of silica powder corresponds to a strain of about 2.5%, while the inflection point of the sample with 10% of silica powder corresponds to a strain of 1.8%. Under the same strain condition, the stress of the sample with a higher proportion of silica powder is smaller (see Fig. 6(a)).

(2) Under the same confining pressure, the Mohr circle corresponding to the sample with a higher proportion of silica powder is smaller, and the sample shows lower strength; the strength envelopes of samples with different proportions of silica powder have similar intercepts on the vertical axis, while the slopes of the envelopes are quite different, indicating that the proportion of silica powder has relatively small influence on the cohesion, while the influence on the internal friction angle is relatively large (see figure 6(b)).

(3) With the increase in the proportion of silica powder (accompanied by the decrease in the proportion of fused quartz), the cohesion and internal friction angle of the sample show a decreasing trend. When the proportion of silica powder increases from 5% to 7%, 10%, and 15%, the cohesion decreases from 54 kPa to 47, 45, and 43 kPa, and the internal friction angle decreases from 41° to 40°, 34. ° and 25° (see Figure 6(c)).

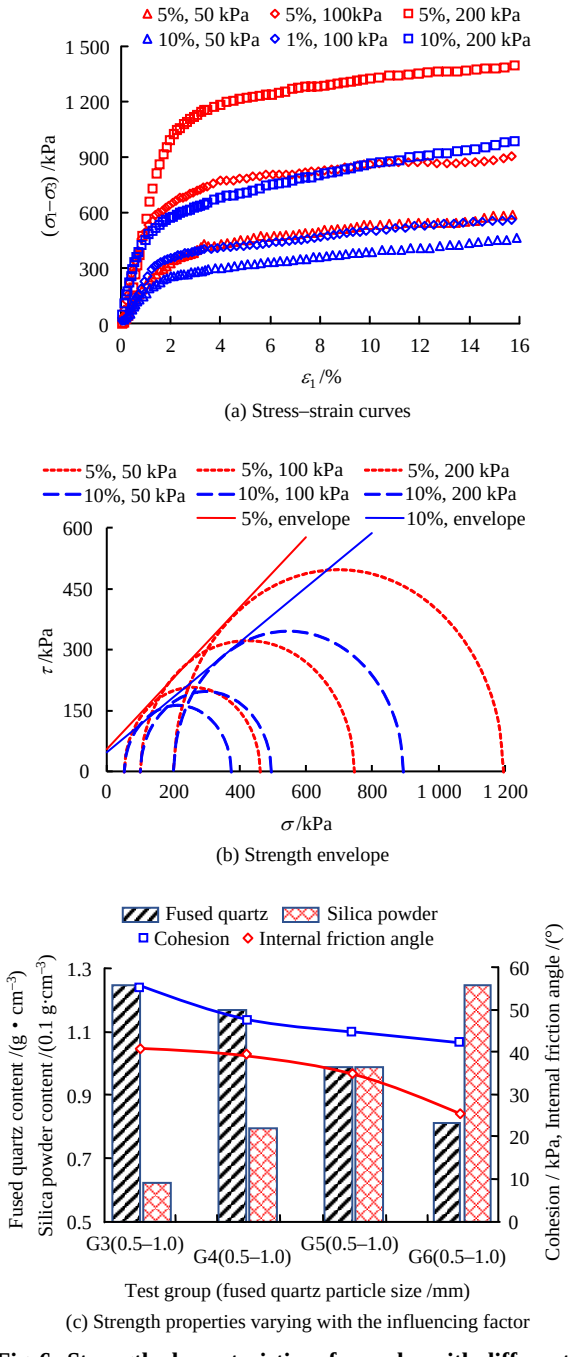

(a) Stress–strain curves

(b) Strength envelope

(c) Strength properties varying with the influencing factor

Fig. 6 Strength characteristics of samples with different proportions of silica powder

4.3 Influence of fused quartz particle size

In the case of constant conditions such as the proportion of silica powder, the degree of compaction and the degree of saturation, the strength characteristics of samples with different fused quartz particle sizes are shown in Fig. 7. In the figure, the three groups of data with the particle size of fused quartz of 0.5–1.0, 0.2–0.5, 1.0–2.0 mm correspond to the G5, G7 and G8 tests in Table 1, respectively. The masses of the fused quartz and silica powder of each sample in these three groups of experiments are the same, only the particle sizes of the fused quartz are different. Therefore, the test groups G5, G7 and G8 constitute a control experiment with the particle size of the fused quartz as a single variable.

From the stress–strain curve (see Fig.7(a)), it can be seen that the shapes and inflection points of the stress–strain curves of the three samples with different particle sizes are basically the same, and under the same strain conditions, the magnitudes of the stress corresponding to the samples with three different particle sizes are as follows: the sample with a particle size of 0.5–1.0 mm has the largest stress, followed by the sample with a particle size of 0.2–0.5 mm, and the sample with a particle size of 1.0–2.0 mm has the smallest stress.

From the strength envelope diagram (see Fig. 7(b)), it can be seen that under the same confining pressure, the sample with the particle size of 0.5–1.0 mm of fused quartz corresponds to the largest Mohr circle, and the sample exhibits a higher strength, followed by the sample with a particle size of 0.2–0.5 mm and the sample with a particle size of 1.0–2.0 mm. There are differences in the intercept of the strength envelope on the vertical axis and the slope of the envelope of the sample with different fused quartz particle sizes, indicating that the particle size of the fused quartz has a certain influence on the cohesion and the angle of internal friction.

It can be seen from the changing pattern of strength parameters (see Fig.7(c)) that among the three different fused quartz particle sizes, the cohesion and internal friction angle of the sample with a particle size of 0.5–1.0 mm are the largest. They are 45 kPa and 34° . The second is the sample with a particle size of 0.2–0.5 mm, and the cohesion and the internal friction angle are 33 kPa and 32° . The smallest is the sample with a particle diameter of 1.0–2.0 mm, the cohesion and internal friction angle are 23 kPa and 31°.

4.4 Influence of fused quartz gradation

In the case of constant conditions such as the proportion of silica powder, the degree of compaction and the degree of saturation, the strength characteristics of the samples with different fused quartz gradations are shown in Fig. 8. In the figure, the three groups of data with the gradation of fused quartz of 0.2–1.0, 0.2–2.0, and 0.5–2.0 mm correspond to the G9–G11 group test in Table 1, respectively. The masses of the fused quartz and silica powder of each sample in these three groups of experiments are the same, only the gradations of the fused quartz are different, so the test groups G9 to G11 constitute a control experiment with the gradation of fused quartz as a single variable.

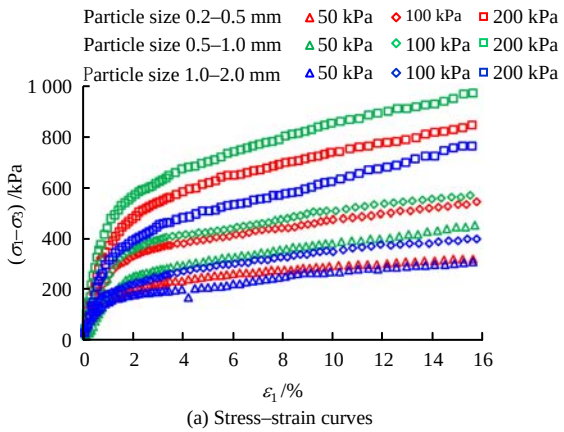

(a) Stress–strain curves

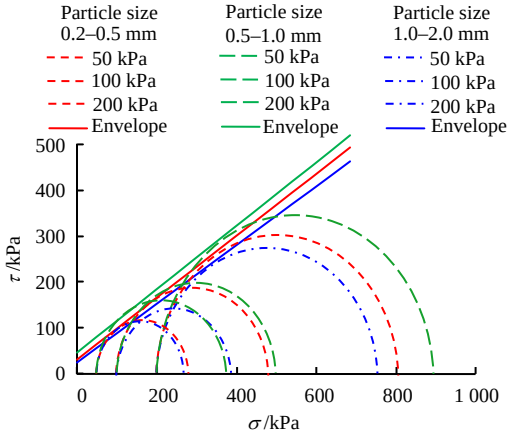

(b) Strength envelopes

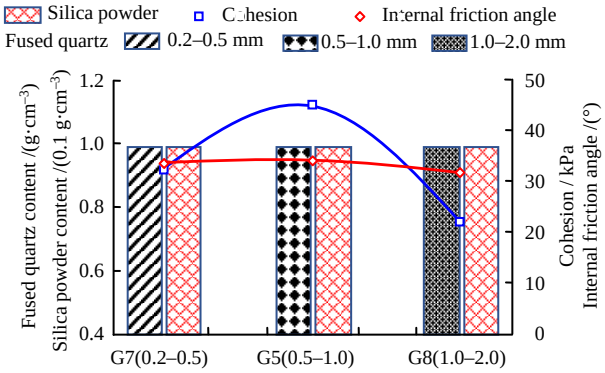

(c) Strength properties varying with the influencing factor

Fig. 7 Strength characteristics of samples with different particle size of fused quartz

From the stress–strain curves (see Fig. 8(a)), it can be seen that the shapes and inflection points of the stress–strain curves of the three different graded samples are basically the same, and under the same strain conditions, the magnitudes of the stress corresponding to samples with three different gradation are: the sample with a gradation of 0.2–1.0 mm has the highest stress, followed by a sample with a gradation of 0.5–2.0 mm, and the sample with a gradation of 0.2–2.0 mm has the smallest stress. The difference in the magnitude of the stress is significant under the lower confining pressure (50 kPa), but not obvious under the higher confining pressure (200 kPa).

From the strength envelope diagram (see Fig. 8(b)), it can be seen that under the same confining pressure, the sample with the fused quartz gradation of 0.2–1.0 mm corresponds to the largest Mohr circle, and the sample shows a higher value of strength, followed by the sample with a gradation of 0.5–2.0 mm and the sample with a gradation of 0.2–2.0 mm; the intercepts of the strength envelopes on the vertical axis and the slopes of envelope curves of the samples with different fused quartz gradations are all different, indicating that the fused quartz gradation has a certain influence on the cohesion and internal friction angle.

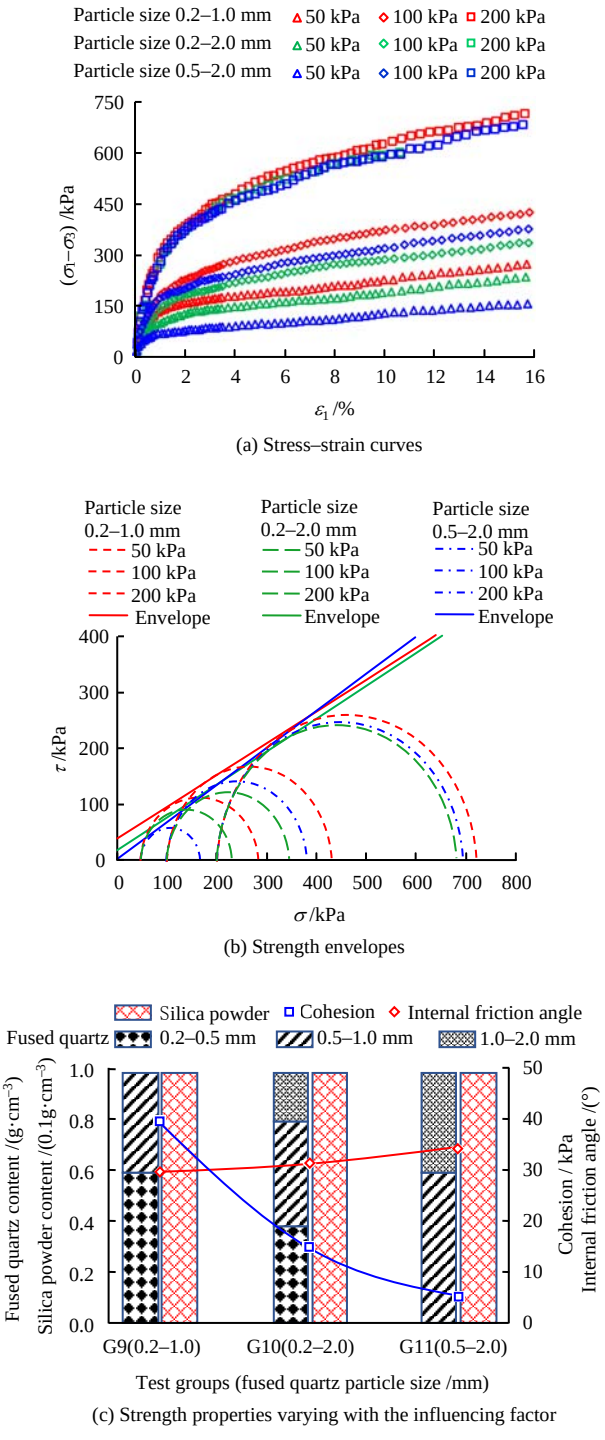

Fig. 8 Strength characteristics of samples with different particle gradation of fused quartz

From the changing pattern of strength parameters (see Fig. 8(c)), it can be seen that among the three different fused quartz gradations, the cohesion of the sample with 0.2–1.0 mm gradation is the largest (39 kPa), and the internal friction angle is the smallest (30°); the cohesion and internal friction angle of the sample with a gradation of 0.2–2.0 mm are of medium size, which are 15 kPa and 31°, respectively; the sample with a gradation of 0.5–2.0 mm has the smallest cohesion (5 kPa), and the internal friction angle is the largest (34°). In general, different fused quartz gradations have a greater impact on the cohesion of these three groups of samples but have less impact on the internal friction angle.

4.5 Comprehensive analysis of influencing factors

A single variable analysis on the influencing factors of transparent cemented soil is made in sections 4.1 to 4.4. In addition, if we perform a comprehensive comparison of Figs. 5 (c), 6 (c), 7 (c) and 8 (c), it can be observed:

(1) When the content of fused quartz is the same (as shown in Fig. 5(c), Fig.7(c) or Fig.8(c)), the particle size, gradation and silica powder content of fused quartz mainly affect the cohesion of the sample (the maximum range of influence is about 35 kPa), whilst it has a smaller influence on the internal friction angle of the sample (the maximum range of influence is about 5°).

(2) The higher the fused quartz content, the greater the internal friction angle of the sample. For example, the internal friction angle of the sample is 38°–44° when the fused quartz content is 1.378 g/cm^3 (see Fig. 5(c)). The internal friction angle of the sample is 30°–34° when the fused quartz content is 0.992 g/cm^3, (see Fig. 7(c) and Fig. 8(c)).

(3) Among the several factors that affect the strength characteristics of transparent cemented soil, the sensitivity of the internal friction angle to the influencing factors is as follows: silica power content (or proportion)> fused quartz particle size> fused quartz gradation, among which fused quartz content (or proportion) is the dominant factor; the sensitivity of cohesion to influencing factors is in order: silica powder content (or proportion)> fused quartz gradation > fused quartz particle size.

4.6 Advantages and applicability

Transparent cemented soil overcomes the defect of transparent sand without cohesion and overcomes the defect of insufficient strength of transparent soft clay. It is a substitute for natural rocks and soils suitable for laboratory model tests. The mechanical properties of transparent cemented soil can be precisely controlled by adjusting the particle size and gradation of fused quartz particles, and the content or proportion of silica powder in the transparent cemented soil, so that it has the ability to simulate a variety of natural rocks and soils.

It can be seen from the stress–strain relationship and strength envelope of transparent cemented soil that the mechanical characteristics of transparent cemented soil are similar to those of natural soils or soft rocks. The changing law of the strength parameters shows that the shear strength parameters of transparent cemented soils

vary widely at varying fused quartz particle sizes (0.2–0.5, 0.5–1.0, 1.0–2.0 mm), gradations (0.2–1.0, 0.2–2.0, 0.5–2.0 mm) and proportions of silica powder (2%–15%), Among them, the cohesion varies from 5 to 65 kPa, and the internal friction angle varies from 25° to 44°. Not only that, it can be predicted that the range of strength parameters of the transparent cemented soil will be further expanded by changing the degree of compactness of the soil. As far as the range of strength parameters of the transparent cemented soil obtained in this article is concerned, the range of strength parameters can covers most of the clay (including loess, expansive soil, soft soil, frozen soil, red clay, saline soil, fill)[28] and some soft rocks (including mudstone, marl and siltstone)[29–30]. Therefore, the transparent cemented soil can be used as a substitute for natural clays and soft rocks in model tests.

5 Conclusion

In this paper, a transparent cemented soil is synthesized with fused quartz as the soil skeleton, nano-level hydrophobic fumed silica powder as the cement, and a mixed mineral oil of n-dodecane and #15 white oil as the pore fluid. Eleven sets of triaxial shear tests were carried out on the four main factors that affect the strength characteristics of the transparent cemented soil, including the amount of soil skeleton and cement. The changing law of the strength characteristics of the transparent cemented soil varying with the content of the cement, the particle size and gradation of the soil skeleton is obtained. Some conclusions are drawn as follows:

(1) Transparent cemented soil with a cohesion of 5–65 kPa and an internal friction angle of 25°–44° can be prepared by appropriately grading fused quartz with particle size of 0.2–0.5, 0.5–1.0, 1.0–2.0 mm, and adding 2%–15% silica powder and its corresponding mixed mineral oil.

(2) When the particle size and gradation of the fused quartz are constant, the internal friction angle of the transparent cemented soil increases significantly with the increase of the fused quartz content, and the cohesion increases significantly with the increase of the silica powder content.

(3) When the content of fused quartz and silica powder is constant, the cohesion of transparent cemented soil is more sensitive to changes in the particle size and gradation of fused quartz, while the internal friction angle is not sensitive to the particle size and gradation of fused quartz.

(4) The stress–strain relationship of transparent cemented soil is similar to those of clays and soft rocks, and its mechanical properties can be precisely controlled by adjusting the content and proportion of silica powder, and the particle size and gradation of fused quartz. The transparent cemented soil can be used in the transparent soil technology to simulate natural clays and soft rocks in visual physical model tests.

References

[1] WHITE D J, TAKE W A, BOLTON M D. Soil deformation measurement using particle image velocimetry (PIV) and photogrammetry[J]. Geotechnique, 2003, 53(7): 619–631.

[2] SADEK S, ISKANDER M G, LIU J. Accuracy of digital image correlation for measuring deformations in transparent media[J]. Journal of Computing in Civil Engineering, 2003, 17(2): 88–96.

[3] SUI Wang-hua, GAO Yue, LIU Jin-yuan. Status and prospect of transparent soil experimental technique[J]. Journal of China Coal Society, 2011, 36(4): 577–582.

[4] ISKANDER M, BATHURST R J, OMIDVAR M. Past, present, and future of transparent soils[J]. Geotechnical Testing Journal, 2015, 38(5): 393–401.

[5] ISKANDER M G, LIU J, SADEK S. Transparent amorphous silica to model clay[J]. Journal of Geotechnical and Geoenvironmental Engineering, 2002, 128(3): 262–273.

[6] PINCUS H J, ISKANDER M G, LAI J, et al. Development of a transparent material to model the geotechnical properties of soils[J]. Geotechnical Testing Journal, 1994, 17(4): 425–433.

[7] ISKANDER M. Transparent soils to image 3D flow and deformation[C]//Proceedings of the Imaging Technologies. [S. l.]: [s. n.], 1998.

[8] WU Ya-jun, LI Jun-peng, JIANG Hai-bo, et al. Consolidation and permeability characteristics of transparent clay with different grain composition[J]. Journal of Northeastern University (Natural Science), 2020, 41(6): 875–880.

[9] LEI Hua-yang, LIU Ying-nan, ZHAI Sai-bei, et al. Visibility and mechanical properties of transparent clay[J]. Chinese Journal of Geotechnical Engineering, 2019, 41(Suppl.2): 53–56.

[10] JIANG Hai-bo, WU Ya-jun, KONG Gang-qiang, et al. Transparent soil model test of vacuum preloading method on ultra-soft soil and formation mechanism of soil pile[J]. Journal of Harbin Institute of Technology, 2020, 52(2): 33–40.

[11] GONG Quan-mei, ZHOU Jun-hong, ZHOU Shun-hua, et al. Strength property and feasibility test of transparent soil to model clayey soil[J]. Journal of Tongji University (Natural Science), 2016, 44(6): 853–860.

[12] ISKANDER M G, SADEK S, LIU J. Optical measurement of deformation using transparent silica gel to model sand[J]. International Journal of Physical Modelling in Geotechnics, 2002, 2(4): 13–26.

[13] SADEK S, M.G I, LIU J. Geotechnical properties of transparent silica [J]. Canadian Geotechnical Journal, 2002, 39(1): 111–124.

[14] KONG Gang-qiang, LIU Lu, LIU Han-long, et al. Triaxial tests on deformation characteristics of transparent glass sand[J]. Chinese Journal of Geotechnical Engineering, 2013, 35(6): 1140–1146.

[15] KONG Gang-qiang, LIU Lu, LIU Han-long, et al. Comparative analysis of the strength characteristics of transparent glass sand and standard sand[J]. Journal of Building Materials, 2014, 17(2): 250–255.

[16] ZHOU Dong, LIU Han-long, ZHANG Wen-gang, et al. Transparent soil model test on the displacement field of soil around single passive pile[J]. Rock and Soil Mechanics, 2019, 40(7): 2686–2694.

[17] ZHOU Hang, YUAN Jing-rong, LIU Han-long, et al. Model test of rectangular pile penetration effect in transparent soil[J]. Rock and Soil Mechanics, 2019, 40(11): 4429–4438.

[18] ZHANG Jia-qi, LI Shu-cai, ZHANG Qing-song, et al. Experimental research on destruction characteristics of tunnel mud inrush using transparent soils[J]. China Journal of Highway and Transport, 2018, 31(10): 177–189.

[19] MA Zhong-wu, SUN Ji-zhu, LIU Jia-jia. Stability of tunnel excavation surface based on experiments of transparent soil[J/OL]. Rock and Soil Mechanics, 2020, 41(Suppl.2): 1–5.

[20] SUI W, ZHENG G. An experimental investigation on slope stability under drawdown conditions using transparent soils[J]. Bulletin of Engineering Geology & the Environment, 2018, 77(3): 977–985.

[21] MAGHSOUDI M S, CHENARI R J, FARROKHI F. A multilateral analysis of slope failure due to liquefaction-induced lateral deformation using shaking table tests[J]. SN Applied Sciences, 2020, 2(8): 1427.

[22] LIANG Yue, CHEN Peng-fei, LIN Jia-ding, et al. Pore flow characteristics of porous media based on transparent soil technology[J]. Chinese Journal of Geotechnical Engineering, 2019, 41(7): 1361–1366.

[23] WU Ya-jun, HAN Ya-dong, TANG Xin, et al. Experiment and numerical simulation of transparent soil migrated by high pressure rotary spray repairing medicament in contaminated soil[J]. Journal of Tongji University (Natural Science), 2020, 48(5): 645–652.

[24] ZHANG Yi-ping, LI Liang, WANG Si-zhao. Experimental study on pore fluid for forming transparent soil[J]. Journal of Zhejiang University (Engineering Science), 2014, 48(10): 1828–1834.

[25] KONG Gang-qiang, SUN Xue-jin, LI Hui, et al. Effect of pore fluid on strength properties of transparent soil[J]. Chinese Journal of Geotechnical Engineering, 2016, 38(2): 377–384.

[26] WEI L, XU Q, WANG S, et al. Development of transparent cemented soil for geotechnical laboratory modelling[J]. Engineering Geology, 2019, 262: 105354.

[27] WEI L, XU Q, WANG S, et al. The morphology evolution of the shear band in slope: insights from physical modelling using transparent soil[J]. Bulletin of Engineering Geology and the Environment, 2020, 79(4): 1849–1860.

[28] CHEN Zheng-hua, GUO Nan. New developments of mechanics and application for unsaturated soils and special soils[J]. Rock and Soil Mechanics, 2019, 40(1): 1–54.

[29] LIU Yong-li, ZHOU Wen-zuo, GUO Bin, et al. Study on marl similar materials in similar simulation test[J]. Chinese Journal of Rock Mechanics and Engineering, 2020, 39(Suppl.1): 2795–2803.

[30] LI Hang-zhou, LIAO Hong-jian. Experimental study on nonlinear strength deformation characteristics of expansive mudstone[J]. Chinese Journal of Underground Space and Engineering, 2007, 3(1): 19–22.